Polarization Switching to the Gain Disfavored Mode in Vertical-Cavity Surface-Emitting Lasers

Markus Sondermann, Michael Weinkath, and Thorsten Ackemann, *Member, IEEE*

***Abstract*—We report on the experimental observation of current-induced polarization switching in vertical-cavity surface-emitting lasers which is accompanied by a decrease of the total output power at the switching point. The relaxation oscillation frequency also decreases. This switching is interpreted as a switching event from the mode with higher (unsaturated) net gain to the gain disfavored mode. The experimental observations are in qualitative agreement with a nonlinear dynamical model taking into account spin degrees of freedom of carriers in a semiconductor quantum well. Within the framework of this model, we propose an explanation for the origin of a minimum in the effective dichroism observed at the switching point, which might also be relevant for other experiments.**

***Index Terms*—Polarization dynamics, vertical-cavity surface-emitting lasers.**

I. Introduction

VERTICAL-CAVITY surface-emitting lasers (VCSELs) have become devices of industrial interest over the past years and are used in an increasing number of applications despite the fact that some aspects of the underlying physics is not yet fully understood. Compared to edge-emitting semiconductor lasers, their main advantages from a point of view of applications are the single longitudinal mode operation, which is enforced by the short cavity length and a circular geometry of the cavity. The latter feature facilitates coupling into optical fibers but also adds additional degrees of freedom to the system, since the orientation of the polarization direction of the emitted field is no longer fixed by geometrical constraints.

Nevertheless, in most cases, a linearly polarized field mode is emitted at lasing threshold. Preferentially, the field vector is oriented along one of the wafer axes [1]. This is due to unavoidable linear polarization anisotropies induced by the elastooptic [1], [2] and the electrooptic effect [3] which break the circular transverse symmetry of the laser. The induced amplitude anisotropy, often termed dichroism, selects the polarization of the lasing mode at threshold in most cases, i.e., for a sufficiently high magnitude of the amplitude anisotropy [4], [5]. In addition, the phase anisotropy or birefringence removes the frequency degeneracy of orthogonally polarized fields, i.e., the orthogonal polarization directions are emitted in modes of the same longitudinal order but with slightly different frequencies. It has been shown that the linearly polarized mode selected at threshold can become unstable at higher injection currents. This can result in polarization switching (PS), i.e., a sudden change of the emission to the orthogonally polarized mode [1], [6]. PS has been observed from the mode with the lower optical frequency to the mode with the higher one and vice versa [1], [6]–[8].

There have been several attempts to explain the mechanisms inducing the PS. One class of approaches is based on thermal effects, which are inevitable during CW operation due to ohmic heating. This results in a different amount of red shift for the cavity resonances and the gain curve and thus in a change of the gain difference between the frequency-separated polarization modes [1]. Further proposals have been made in [9] and [8], taking into account also frequency-dependent losses or strain effects in the quantum-well (QW) active region, respectively. Common to all of these models is that they explain PS by a current-dependent change of the *linear, i.e., unsaturated, net gain anisotropy* that becomes zero and changes its sign at the point of the PS.

A different approach is based on the nonlinear dynamics induced by saturable dispersion and the coupling of inversion populations with opposite spin [10], [11]. In this model, PS occurs due to a phase instability, i.e., a change of the phase relationship of the left- and right-handed circular polarized components of the emitted light. An important prediction of this model is that PS from the mode favored by the net gain to the gain disfavored mode is possible. In [12] and [13], this model has been extended by introducing a frequency-dependent susceptibility, which gives a more realistic description of the semiconductor gain medium than the quasi-two-level approach used in [10] and [11]. The extended model allows for a combined investigation of nonlinear and temperature-dependent linear effects.

From an experimental point of view, the question is how to differentiate among the proposed mechanisms. One approach is to operate the laser with current pulses with a duration far below the thermal relaxation times. A PS from the mode with higher optical frequency to the mode with lower optical frequency (often referred to as "type I PS" [9]) under pulsed operation has been observed in [14] and in [15]. However, it was argued that this does not give conclusive evidence for a nonthermal switching, since the plasma temperature might change even if the lattice temperature remains constant [16].

Another possibility is to look for "fingerprints" of the nonlinear dynamics. The model proposed in [11] predicts for the PS from the mode with lower optical frequency to the mode with higher optical frequency ("type II PS" in the terminology of [9]) the occurrence of elliptically polarized dynamical states

Manuscript received April 2, 2003; revised October 23, 2003. This work was supported by the Deutsche Forschungsgemeinschaft and the Deutsche Akademische Austauschdienst.

The authors are with the Institut für Angewandte Physik, Westfälische Wilhelms–Universität Münster, D–48149 Münster, Germany (e-mail: sondema@uni-muenster.de; t.ackemann@uni-muenster.de).

Digital Object Identifier 10.1109/JQE.2003.821537

at the PS, which lead to a reduction of the fractional polarization and appear as sidebands in the optical spectrum. The possibility of the existence of this PS scenario has been experimentally demonstrated in [17]. Within the framework of the above model, characteristic spectra or similar phenomena are not predicted for type I PS. Therefore, one has to look for other manifestations of the switching to a mode with lower net gain.

In this paper, we report on a possibility of identifying experimentally a type I switching event as a PS to the gain disfavored mode. This is possible by the observation of a decrease of the output power of the laser at the point of PS. We will also argue that the observation of a minimum of the dichroism at the point of PS, reported for type I switching in [7], is—taken alone—not sufficient to distinguish between switching processes due to a change of linear (unsaturated) or nonlinear net gain. In [7], this minimum has been interpreted as the consequence of a sign reversal of the linear dichroism. Here, we discuss another possible origin of a minimum in the dichroism. We will show that, within the theory of [11] and [13], such a minimum is also obtained and is the consequence of nonlinear dynamics in the regime of low spin relaxation rates. We mention that the relevance of the spin degrees of freedom of the gain material for polarization selection has been studied intensively in gas lasers (see [18] for a review). In this context, the possibility of a switching to a gain disfavored mode is an established—though somehow counterintuitive—concept. It can be due to an interplay of birefringence and phase-amplitude coupling in *detuned* gas lasers [11], [18]–[20]. Since in semiconductor lasers phase-amplitude coupling is particularly strong and, in addition, exists even for operation at the gain peak [21], the existence of similar effects in VCSELs is not totally surprising.

In Section II, we will describe the experimental setup and report the results of our experiments. In Section III, we will compare these results to simulations and a linear stability analysis within the model established in [12] and [13]. A discussion and conclusions will be given in the last section.

II. Experiments

The experiments have been performed on gain-guided VCSELs (Emcore Corp., Model 8085–2010) with an 8-μm-wide aperture. The devices operate in the fundamental transverse mode for current values less than 200% of the threshold current. The operation wavelength is around 845 nm. The substrate temperature of the VCSELs has been stabilized by a thermoelectric cooling system that has been attached to the copper mount of the VCSELs. With this system we are able to monitor and control the substrate temperature in a range from 6 °C to 70 °C, where the upper limit is set by the maximum allowed operation temperature of the devices used.

The VCSEL emission has been collimated using an aspheric antireflection coated lens. After collimation, the emitted light is split into its orthogonally linear polarized components by means of a half-wave plate and a Wollaston prism. For projection onto circular polarization states, a quarter-wave plate is inserted into the beam path in front of the half-wave plate. All polarization optics have been slightly misaligned in order to prevent feedback into the laser. After the Wollaston prism, the time-averaged power in each polarization component is measured with a low-bandwidth detector. We have measured power spectra with a PIN diode of 10-GHz bandwidth (Antel AR-S2) and a power spectrum analyzer of 21-GHz bandwidth (Anritsu MS2650). A scanning Fabry–Perot interferometer with a finesse better than 150 and a free spectral range of 46 GHz allows for a measurement of optical spectra. Unintended back reflections from the Fabry–Perot interferometer and the PIN diode are prevented by an optical isolator.

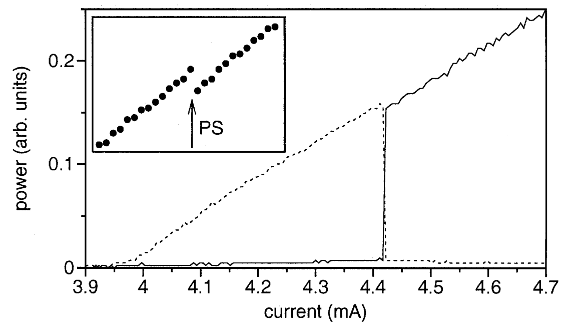

Fig. 1. Polarization-resolved output power in dependence of the injection current. Solid (dashed) lines denote the power in the polarization direction corresponding to the mode with lower (higher) optical frequency. The inset displays a magnification of the total output power (dotted line) in the vicinity of the PS, measured without polarization-sensitive optics.

Fig. 1 displays the polarization resolved output power in dependence of the injection current (LI-curve) under CW operation for one of the investigated devices. At lasing threshold the light is emitted in the mode with higher optical frequency. This has been confirmed by measurements of the optical spectrum, revealing a frequency splitting of the two modes at threshold of approximately 6 GHz. A PS to the mode with lower optical frequency is observed at 11% above the threshold current. At the PS, a small decrease of the output power of approximately 3% is observed, i.e., the mode with lower optical frequency has a lower emission power than the orthogonally polarized mode at the point of the PS. A linear interpolation of the power of the mode with lower optical frequency intersects the current axis at a current value that is higher than the lasing threshold, which is the threshold of the mode with higher optical frequency. This indicates that the threshold of the mode with lower optical frequency is higher.

In order to ensure that the observed decrease of power is not due to a residual anisotropy of the analyzing polarization optics, we have placed a low-bandwidth detector directly after the collimation lens. The total output power obtained from this measurement exhibits a abrupt decrease at the PS in accordance with the polarization-resolved experiments (see the inset in Fig. 1).

An additional tool to visualize the observed decrease in power is a measurement of the relaxation oscillation (RO) frequencies for the orthogonally polarized modes. The square of the RO frequency is—in linear approximation—expected to be proportional to the output power or the injection current rescaled to the threshold current [22], respectively. The advantage of this method from the experimental point of view is that the frequency of the RO is not changed by potential polarization anisotropies in the experimental detection system. In Fig. 2, the measured squared RO frequency is plotted in dependence of the

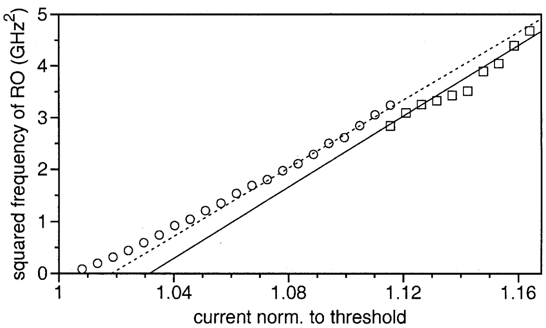

Fig. 2. Square of RO frequency against the injection current. Circles (squares) denote the relaxation oscillation frequency before (after) the PS. The dashed and solid lines are the results of linear fits applied to the two datasets.

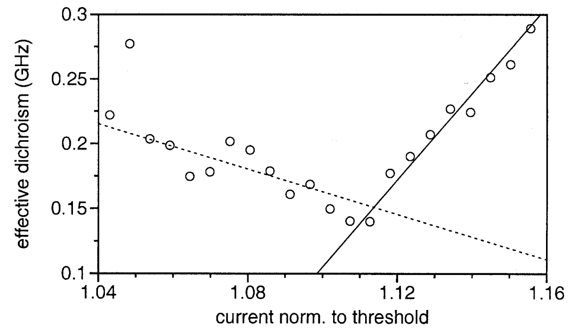

Fig. 3. Effective dichroism in dependence on the injection current. The dashed (solid) lines are linear fits applied to the data before (after) the PS.

current. At the point of PS, the square of the frequency decreases stepwise. In addition, the results of linear fits applied to the data before and after the PS intersect the current axis at different currents. This is a further indication of different thresholds of the two modes, i.e., of a higher threshold of the mode with lower optical frequency.

As is apparent from Fig. 2, the square of the RO frequency has no strict linear dependence on the current close to threshold. This is observed for all of the devices we have investigated, regardless of the state of polarization selected at threshold and whether a PS occurs or not. The range of data points included in the fitting procedure has been restricted to the linear part, i.e., to current values greater than 6% above threshold. The origin of the deviation is not understood but might be due to the fact that in gain-guided devices the modal parameters and modal volume depend on current due to thermal lensing.

In [7], two different methods have been established to measure the frequency and the damping of a perturbation that is orthogonally polarized to the lasing mode and driven by spontaneous emission. In experiments, this perturbation appears as the nonlasing mode in the optical spectrum. The frequency and the width of this peak are related to the effective phase and amplitude anisotropies which stem from linear and nonlinear (dynamical) contributions [7], [23]–[25] and are often called effective birefringence and effective dichroism, respectively. They can be measured as the difference in frequency and the difference in linewidth [half-width at half-maximum (HWHM)] of the lasing and the nonlasing mode in the optical spectrum. A second, more precise method is the analysis of polarization fluctuations in RF spectra [7]. The polarization fluctuations are observable after projection onto circularly polarized states. The center frequency of the peak in the noise spectrum corresponds to the oscillation frequency of the orthogonally polarized perturbations (effective birefringence) and the HWHM to the damping of these perturbations (effective dichroism) [7].

The results of the latter method applied to the device under study are displayed in Fig. 3. The effective dichroism exhibits a minimum at the point of the PS. Linear fits applied to the data before and after the PS reveal that the modulus of the slope of the effective dichroism after the PS is larger than the one before the PS. Similar experimental results are displayed in [7, Fig. 10].

The scenario described up to now is observed for substrate temperatures of the VCSEL ranging from 6 °C to 55 °C. The latter value is in the vicinity of the threshold minimum of the studied device. Thus, the PS is observed in a temperature range of almost 50 °C. The increase of the active zone temperature with current varies from 3 °C to 4 °C/mA. These values have been obtained by a comparison of the redshift of the lasing mode for increasing current at constant substrate temperature and the redshift for increasing temperature at a constant injection current. The observed PS occurs at current values less than 1 mA above the lasing threshold. This is an indication that the PS observed in this VCSEL is not due to temperature changes. A PS from the mode with higher optical frequency to the mode with lower optical frequency exhibiting a drop of output power has been observed also for other devices in our experiments.

III. Theoretical Investigations

In [12] and [13], an extension of the spin flip model established in [11] is introduced. Whereas in [11] the semiconductor material has been modeled as a two-level medium, i.e., only transitions in the center of the band gap have been taken into account, in [12] and [13] a more realistic semiconductor susceptibility [26] is used to model the properties of the gain material. An important issue of this susceptibility is the dependence on a detuning (Δ) between the cavity resonance and the nominal bandgap. This opens the possibility of modeling detuning-dependent gain differences of the two polarization modes and hence the temperature effects on detuning identified in [1] and [4] as a possible reason for type I PS in VCSELs. For an exact expression of the susceptibility, we refer to [13] and [26]. The dynamical equations describing the evolution of the circularly polarized field components $E_\pm$ and the corresponding inversion populations with opposite spin $D_\pm$ are [13]:

$$\begin{aligned}\dot{E}_\pm(t) =& -\kappa E_\pm + i\frac{a\Gamma}{2}\chi_\pm\left(\Omega + i\frac{\dot{E}_\pm}{E_\pm}, D_+, D_-\right)E_\pm \\ & - (\gamma_a + i\gamma_p)E_\mp + \sqrt{\beta_{\rm sp}D_\pm}\xi_\pm(t)\,, \qquad (1)\\ \dot{D}_\pm(t) =& \frac{\mu}{2} - AD_\pm - BD_\pm^2 \mp \gamma_j(D_+ - D_-) \\ & + a\cdot Im\chi_\pm\left(\Omega + i\frac{\dot{E}_\pm}{E_\pm}, D_+, D_-\right)|E_\pm|^2. \qquad (2)\end{aligned}$$

The important parameters that influence the dynamics are the dichroism γ_a, the birefringence γ_p, and the spin relaxation rate γ_j. γ_a is set to zero. By this, the VCSEL is able to emit in the high-frequency mode at threshold for detuning values less than

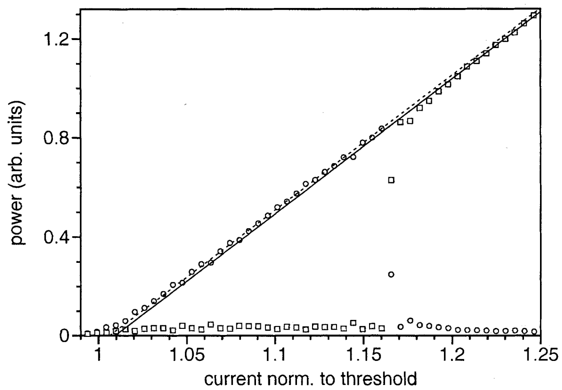

Fig. 4. Same as Fig. 1, obtained from simulations for $\Delta = 0$. Circles (squares) denote the power in the mode with higher (lower) optical frequency. The dashed (solid) lines are linear fits applied to the data before (after) the PS. The integration time per point is 100 ns.

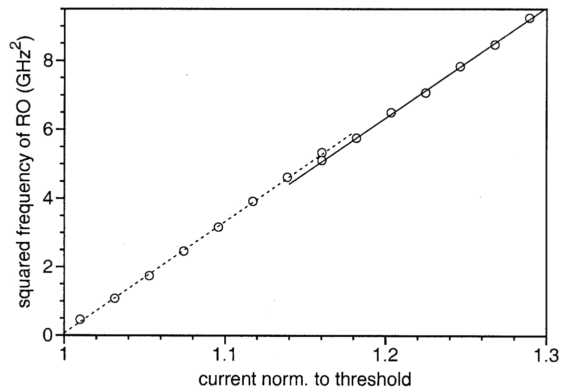

Fig. 5. Same as in Fig. 2, obtained from simulations with $\Delta = 0$ and an integration time of 1000 ns per point. The dashed (solid) lines are linear fits applied to the data before (after) the PS.

the one of the threshold minimum [13], which is located in the simulations at $\Delta = 0.65$. (The definition of Δ and the semiconductor material properties included in the calculation of the susceptibility [26] result in a shift of the threshold minimum away from zero detuning.) Since γ_a is a pure loss anisotropy independent of Δ, the net gain anisotropy at threshold is a function of the detuning Δ. To operate under conditions close to the experimental conditions, γ_p is set to 18 ns^{-1}. The mode splitting at threshold in optical frequencies is roughly γ_p/π. The crucial parameter is the relaxation rate γ_j of the difference of the inversion populations with opposite spin. Since we want to demonstrate the importance of these relaxation processes, we choose a value of $\gamma_j = 20\ \text{ns}^{-1}$, which is comparable in magnitude to the birefringence. The remaining parameters of the above equations and the corresponding values used in the simulations are the cavity losses $\kappa = 300\ \text{ns}^{-1}$, the effective gain constant $a = 2.3 \cdot 10^4\ \text{ns}^{-1}$, the confinement factor $\Gamma = 0.045$, the nonradiative and bimolecular recombination rates of the carriers $A = 0.5\ \text{ns}^{-1}$ and $B = 1.0\ \text{ns}^{-1}$, respectively, and the spontaneous emission rate $\beta_{\text{sp}} = 10^{-6}\ \text{ns}^{-1}$. Spontaneous emission processes are incorporated by the two Gaussian white noise sources $\xi_{\pm}$. μ is the injection current normalized to the transparency carrier density.

The linearly polarized steady-state solutions of (1) and (2) have an equal amplitude and frequency for the $E_{\pm}$-fields but a different phase at which the circularly polarized components lock [13]. The steady-state inversions of the orthogonally linear polarized solutions are functions of γ_a and the imaginary part of the susceptibility. This results in general in different thresholds for the two polarization modes and in different amplitudes of the linearly polarized fields at constant current [13]. Furthermore, in a linearly polarized steady state, one has $D_+ = D_-$, i.e., the difference of carriers with opposite spin has relaxed to zero [13].

In Fig. 4, the simulated L–I curve for a detuning value of $\Delta = 0$ is displayed. At threshold, the laser oscillates in the polarization mode with higher optical frequency, which is the one closer to the gain peak. If the current is increased beyond a value of 16% above the lasing threshold, a PS to the mode with lower optical frequency is observed. The value of 16% is of the same order of magnitude as the one observed in the experiment. An even better agreement can be obtained by decreasing γ_j by a small amount or by choosing a value for the detuning closer to the minimum threshold condition. However, a further fine tuning of parameters for achieving "perfect" agreement does not appear to be fruitful, since too many unknown parameters are involved. Hence, we prefer to demonstrate only the robust features assuming reasonable parameters.

Linear fits have been applied to the data before and after the PS (see the lines in Fig. 4). The fitting results reveal, as expected from the steady-state characteristics [13], a drop of the output power at the PS and a higher threshold for the mode with lower frequency, i.e., the PS is to the mode with lower gain. The decrease of power at the PS is of the order of 2%.

Under typical experimental conditions, i.e., CW operation of the VCSEL, the temperature of the active zone increases with the injection current due to ohmic heating. Thanks to the frequency-dependent susceptibility used in the model discussed here, one is able to simulate an increasing temperature of the active material by increasing Δ proportional to the injected current [13]. This procedure has been applied to the same parameter set as it was used for the simulation in Fig. 4, with the initial value of the injection current being a few percent below the threshold current for fixed detuning. As long as the increase of Δ with current is moderate, i.e., the drift in Δ does not significantly modify the threshold current, the drop of the output power at the PS is still observed. For simplicity, we will keep to the investigation of the dynamics at constant detuning $\Delta = 0$ in the following.

As a next step, simulations of the polarization-resolved output power at constant current over a period of 1000 ns have been performed. The power spectra obtained by a numerical Fourier transformation of the time traces of the output power have been fitted to Lorentzian functions in order to obtain the RO frequencies. The results of this procedure are displayed in Fig. 5. At the current of the PS, the RO for both modes are observed, since in the vicinity of the PS noise-driven mode hopping occurs (see also [27]–[29]). Thus, both modes are lasing on a time average. As is evident from the figure, there is a drop of the squared RO frequency at the PS point. This matches the experimental observation. The drop in RO frequency is due to the drop in intracavity power (and correspondingly of the output power, of course).

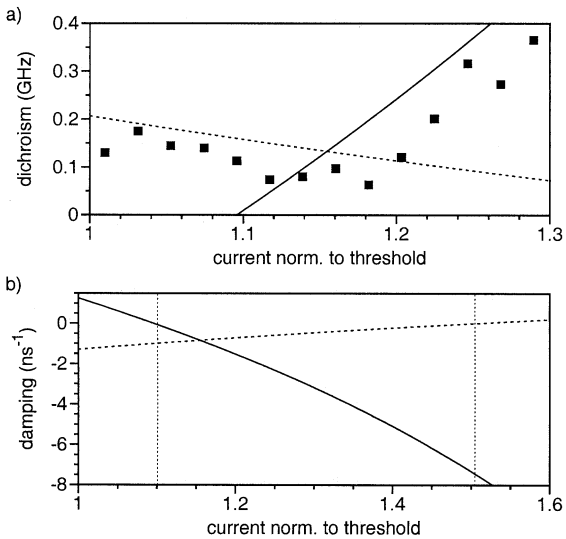

Fig. 6. (a) Effective dichroism in dependence on the injection current for $\Delta = 0$, obtained from simulated optical spectra. (b) Damping (in angular frequencies) of the perturbation orthogonally polarized to the lasing mode, obtained from a linear stability analysis. The dashed (solid) lines in (b) denote the perturbation orthogonally polarized to the mode with higher (lower) optical frequency. The dotted lines indicate the current interval of linear bistability of the two polarization modes. The lines in (a) represent the modulus of the corresponding data in (b), divided by a scaling factor of 2π.

In Fig. 6(a), the difference in linewidth (HWHM) of the peaks of the two polarization modes in simulated optical spectra, i.e., the effective dichroism, is plotted as a function of the injection current. This is a measure for the damping of a perturbation that is orthogonally polarized to the lasing mode and driven by spontaneous emission (see [7], [25], and Section II). For the case of lasing emission in the mode with higher optical frequency, a decrease of the damping (and hence of the dichroism) is observed, whereas it increases after the PS when the mode with lower optical frequency lases. Thus, the effective dichroism has a minimum at the PS (16% above threshold) in accordance with the experimental observations. Moreover, the slope of the damping before and after the PS exhibits the same characteristics as for the experimental data, i.e., the modulus of the slope increases after the PS.

In the remainder of this section, we will compare the results of the simulations with the predictions of a linear stability analysis describing the stability of the two linearly polarized steady-state solutions against perturbations with perpendicular polarization. The stability of the lasing mode against these perturbations is expressed by three eigenvalues, of which one is real and the other two are complex conjugate, as is also the case in the original model [11], [24]. For the parameter values discussed here and current ranges less than twice the threshold current, the real eigenvalue is always negative. Hence, the discussion can be restricted to the two complex conjugate eigenvalues. These describe the development of the perturbations at the orthogonal polarization mode. The real part of the eigenvalues describes the (un)damping of a perturbation, where for a positive (negative) real part the perturbation grows (decays) exponentially in time, i.e., the solution subject to the perturbation is linear unstable (stable).

In Fig. 6(b), the numerically obtained results of a linear stability analysis for the same parameter set as used in the simulations are displayed. At threshold, only the solution for the mode with higher optical frequency is stable. For increasing current, the solution for the mode with lower optical frequency gains linear stability at approximately 10% above threshold. The mode with higher optical frequency loses its stability at 50% above the lasing threshold. This is the point at which the PS would be expected to occur from the point of view of linear stability. Since the modulus of the damping of the perturbation can be measured as the effective dichroism [7], one would expect a continuous decay of the effective dichroism toward zero at the PS, where a stepwise increase of the effective dichroism should occur. This is obviously not the case in the simulations [see Fig. 6(a)] nor in the experiment. There, the PS is at much lower current and and a nonzero minimum of the effective dichroism is observed.

However, the PS in the simulations does not take place at the upper boundary of the bistability interval (50% above threshold), but at a current value of 16% above threshold. Just slightly below this current value, the damping values corresponding to the stability of the orthogonally polarized lasing solutions cross. This explains the finite value of the minimum of the difference in linewidth of the lasing and the nonlasing mode, as it is observed at the PS in the simulations [Fig. 6(a)]. Since the modulus of the damping of the perturbation to the mode with lower frequency increases faster with current than the damping of the perturbations to the other mode decreases, the slope of the difference in linewidth is steeper after the PS.

Regarding the region of linear bistability of the modes, there has been an apparent contradiction between experimental observations and the models based on spin relaxation processes in the past. In experiments, the PS is often observed to be accompanied by a hysteresis loop (e.g., [7] and [30]), which can be regarded as a manifestation of bistability. The width of the observed hysteresis loops was found to be much smaller than the region of bistability that is obtained here or in [11], [12]. This "contradiction" is resolved by our numerical observation that the point of PS is not at the linear stability boundaries in the presence of spontaneous emission noise. Obviously, the strength of the noise will have some influence on the switching point. For the parameters under study, a change of β_{sp} has the following consequences. If β_{sp} is decreased by, e.g., a factor of 2, the point of PS moves to 28% above threshold. A further decrease of β_{sp} results in a further increase of the switching current, but the relative change of the switching current is the smaller the larger the decrease of β_{sp} is, i.e., there is no proportionality between β_{sp} and the switching current. The point of the PS moves asymptotically toward the current value at which the mode with the higher frequency loses linear stability. On the contrary, if β_{sp} is increased, the switching point remains constant. However, an increase of β_{sp} results in an increase of the current interval in which mode hopping is observed. Thus, the PS as observed in Fig. 4 is smeared out.

We want to finish this section with a discussion of the influence of variations of the spin flip rate on the damping of the perturbations. If all other parameters are fixed, the spin flip rate γ_j determines the slope of the damping of the perturbations with changing current. With increasing γ_j, the slope of the damping of the perturbation orthogonally polarized to the mode with higher (lower) optical frequency decreases (increases). As a consequence, the point at which the mode with lower (higher) optical frequency gains (loses) linear stability moves to higher current values. This in turn results in an increase of the current value at which the damping values of the two solutions intersect. Furthermore, due to the smaller slopes, the minimum of the damping at the intersection point becomes less pronounced. This development continues until for $\gamma_j = 33$ ns^{-1} the slope of the damping that determines the stability of the mode with higher frequency changes its sign. This implies that the mode with higher optical frequency remains linearly stable for all current values, since the real part of the corresponding eigenvalue will always remain negative. This matches the fact known in the literature that type I switching typically does not occur any more, if the spin flip rate is increased for otherwise fixed parameters [11], [31], [32]. Actually, it does not survive at all in a reduction of the spin flip model (SFM) to a class-A laser model [31], [32], though it can be kept in a reduction to a two-mode class-B rate equation model [33].

An increase of γ_j also results in a shift of the PS current in the simulations away from the intersection point of the damping values, if the noise strength is kept constant. The reason is that the two eigenvalues become more equal for increasing γ_j. For $\gamma_j = 30$ ns^{-1}, PS is not observed anymore at current levels less than twice the threshold current, which matches the interval of fundamental transverse mode operation in most gain-guided devices. The shift of the switching point to higher currents with increasing spin relaxation rate can be partly compensated for by an increase of the spontaneous emission noise. The more noise is added in the simulations, the closer the PS moves to the current value where the real parts of the eigenvalues intersect.

For completeness, we want to note that a minimum in the damping of the perturbation to the lasing solutions can also be obtained within the original model. However, we prefer to use the extended version, since we want to be able to mimic a temperature-induced detuning change for cross checking (as discussed above) and since it involves less free parameters. For example, the linewidth-enhancement factor α for semiconductor lasers [21] appears as an additional parameter that has to be properly chosen. In the theory used in this paper, α is not a free parameter. Instead, it results from the susceptibility describing the active semiconductor material [26].

On the other hand, the model discussed in [11] and [34] has the advantage of allowing analytical insight to a large degree. For example, it is known that a PS from the high-frequency mode to the low-frequency mode can only take place for a birefringence larger than [34]

$$\gamma_p > \frac{\gamma_s}{2\alpha} \approx \frac{\gamma_j}{\alpha} \tag{3}$$

where α is the so-called linewidth-enhancement factor describing phenomenologically phase-amplitude coupling in the original SFM [11], [34] and $\gamma_s = 2\gamma_j + \gamma_e$. γ_e is the decay rate of the total carrier population. The right-hand side of the above equation holds true for $2\gamma_j \gg \gamma_e$, which is a reasonable assumption for the value of γ_e stated below and the spin flip rates used here. For the experimental value of $\gamma_p = 18$ ns^{-1} and α of the order of $1 \ldots 5$, it is immediately apparent from (3) that the spin flip rate should not be too high in order to allow for a PS. The switching point versus threshold is given by [34]

$$\mu = 1 + \frac{2\gamma_a}{\kappa} \frac{2\gamma_j^2 + 2\gamma_p^2}{\alpha\gamma_p - \gamma_j} \frac{1}{\gamma_e} \tag{4}$$

where γ_a denotes the net dichroism (now including the gain part) and μ is scaled such that it is zero at transparency and one at threshold (for $\gamma_a = 0$). The meaning of κ and γ_p is as in the extended version of the model. The intensity difference between the linearly polarized states is $\Delta I \approx 2\gamma_a/\kappa$ in the first order of γ_a/κ [11]. Hence, the relative intensity difference (i.e., the intensity difference scaled to the intensity of the lasing mode) is

$$\frac{\Delta I}{I} = \frac{2\gamma_a}{\kappa} \frac{1}{\mu - 1}. \tag{5}$$

By inserting (5) into (4), it is possible to eliminate γ_a/κ and solve for α. Using the experimental values for the parameters where known ($\Delta I/I = 0.03$, $\gamma_p = 18$ ns^{-1}) and the ones assumed in the numerical treatment otherwise ($\gamma_j = 20$ ns^{-1}), one obtains $\alpha \approx 3.5 \ldots 2.7$ for $\gamma_e \approx 1 \ldots 1.5$ ns^{-1}. These are reasonable value for semiconductor quantum wells which are consistent also with (3).

IV. Discussion and Conclusion

The drop of power and RO frequency at the point of the PS observed in the experiments is predicted in simulations based on the model that is discussed in the previous section. In the theory, this drop occurs because the two orthogonal polarization modes have different thresholds. The linear fits applied to the experimentally obtained LI-curves and to the square of the RO frequencies hint to the existence of a higher threshold for the mode with lower optical frequency. Thus, it can be concluded that the experimentally observed polarization switching is from the mode with higher unsaturated net gain to the mode with lower unsaturated net gain.

A further qualitative agreement between experiment and simulations is observed for the development of the effective dichroism. For both simulations and experiment, a minimum of this quantity is observed at the PS. These observations can be explained by the predictions of the linear stability analysis for the lasing mode. Hence, the linear stability analysis seems to be sufficient to describe the damping of the perturbations in the simulations *and* the experiment.

However, the linear stability analysis fails to predict the point of the PS. The point of PS in the simulations coincides with a current value close to the point where the perturbations to the two lasing solutions are equally damped. The laser seems to switch to the mode that is more stable in the sense that orthogonally polarized perturbations are damped more strongly. In the current state of the investigations, a critical value for the difference in damping that is necessary to induce the PS cannot be given. This difference seems to depend on the parameters, in particular on the spin relaxation rate and on the noise strength. Hence, a more complicated mechanism that determines the (nonlinear) stability of the polarization modes needs to be considered.

A minimum in the effective dichroism of the lasing and nonlasing modes has often been observed in previous experimental investigations on type I PS [7], [35]. In [7], this minimum has been found for all PS's of that kind. There, however, this minimum was interpreted to result from a current dependence of the linear dichroism of unknown origin [7], since without such an assumption the effective dichroism cannot exhibit a minimum at the PS, if the spin dynamics are adiabatically eliminated from the SFM equations [7], [32]. In the same limit, type I PS at a constant linear net gain is not possible anymore, since the real part of the eigenvalue describing the stability of the mode with higher optical frequency decreases continuously proportional to the current normalized to threshold. Thus, once the real part is negative, it remains negative, i.e., the mode with higher optical frequency remains linearly stable for all injection currents. This fact provides further justification for the suggestion in [7] of a current dependence of the linear dichroism. However, such a change of sign of the linear dichroism is not compatible with the experimentally observed decrease of power at the PS for the devices investigated in this paper. If the two polarization modes have equal linear (unsaturated) net gain at the switching point, the power in both modes has to be equal (see below for a discussion of gain compression effects).

A possible explanation for the different results obtained here and in [7] is a different spin relaxation rate in the investigated devices. The results in [7] and accompanying papers (see [7] and [32] and the references therein) consistently suggest a rather large spin flip rate ($\gamma_j > 50\ \mathrm{ns}^{-1}$). In that case, type I switching is indeed only possible if a current dependence of the linear net gain is assumed (see the discussion in the previous section). In contrast, for the VCSELs investigated in this paper, the spin flip rate appears to be low. We have tried to determine the spin flip rate from the behavior of the effective dichroism and birefringence versus current by applying the theory assuming adiabatic elimination of spin dynamics developed in [32] in the same way as it was done in [7]. The spin flip rate obtained from this procedure is found to be of equal magnitude to the birefringence, which violates the conditions given in [32] for adiabatic elimination of the spin dynamics. Therefore, we conclude that the experimental results obtained for the VCSELs investigated in this paper can only be described by a model that accounts for spin flip rates that are sufficiently small. This is also in agreement with the fact that experimental results on type II switching [17] and two-mode dynamics for the case of a very small dichroism at threshold [5] can only be reproduced if the spin flip rate is assumed to be low [5], [36]. These results have been obtained for devices of the same type and manufacturer.

Finally, we comment on possible effects of self- and cross-saturation terms (often called also "gain compression" terms, e.g., [22]), i.e., reductions of the unsaturated gain of the x mode due to terms like $1/(1+\epsilon_{xx}|E_x|^2+\epsilon_{xy}|E_y|^2)$ or $1-\epsilon_{xx}|E_x|^2-\epsilon_{xy}|E_y|^2)$ (and vice versa for the y mode, where the subscripts x and y denote the fields and saturation coefficients of the two modes with orthogonal linear polarization). If the cross-saturation terms are introduced by a reduction of the SFM-model to a class-B rate equation system, the features of a drop of power at the PS point and of a switching to a gain disfavored mode are present also in this reduced model, as can be checked explicitly by looking at [33, eqs. (37) and (38)]. In phenomenological models in which the PS is induced by a current dependence of the unsaturated gain (e.g., [7] and [37]), switching takes place toward the gain favored mode by definition. Hence, the LI-curve of total power should be continuous since the gain difference is zero at the PS point. Self- and cross-saturation terms are often introduced in order to explain the observed hysteresis around the PS point [37]. If the self-saturation coefficients are equal for the two polarization modes, there should actually be a jump to higher power (for increasing current) since the switching is delayed. Indeed, there is consensus in the literature that the differences in the self-saturation should vanish (see [38] and [39] for a specific model) or at least be small due to the nearly symmetric structure of the VCSEL [37]. In any case, a difference in the self-saturation coefficients large enough to induce a power drop should be accompanied by a correspondingly large change in the slope of the LI-curve, since self-saturation influences the slope but not the threshold (see [22] and the explicit solutions in [37] and [38]). However, there is no indication for that in the experimentally obtained LI-curves.

In conclusion, we have experimentally demonstrated PS in VCSELs to a mode with lower linear net gain for the case of PS from the mode with higher optical frequency to the mode with lower optical frequency. This PS is manifested by a decrease of the output power and the RO frequency. The PS and the observed minimum of the effective dichroism can be explained theoretically by the model established in [12] and [13], if a sufficiently low spin relaxation rate is taken into account.

Note added in proof: After submission of the manuscript, a paper on optically pumped long-wavelength VCSELs appeared that also reports a drop in output power after a PS [40].

ACKNOWLEDGMENT

The authors gratefully acknowledge the support and encouragement of W. Lange in this work. They also want to thank J. Mulet for the possibility of using his programs for the theoretical investigations and S. Balle for fruitful discussions.

REFERENCES

[1] K. D. Choquette, D. A. Richie, and R. E. Leibenguth, "Temperature dependence of gain-guided vertical-cavity surface emitting laser polarization," *Appl. Phys. Lett.*, vol. 64, pp. 2062–2064, 1994.

[2] A. K. v. Doorn, M. P. van Exter, and J. P. Woerdman, "Elasto-optic anisotropy and polarization orientation of vertical-cavity surface-emitting semiconductor lasers," *Appl. Phys. Lett.*, vol. 69, pp. 1041–1043, 1996.

[3] R. F. M. Hendriks, M. P. van Exter, J. P. Woerdman, A. v. Geelen, L. Weegels, K. H. Gulden, and M. Moser, "Electro-optic birefringence in semiconductor vertical-cavity lasers," *Appl. Phys. Lett.*, vol. 71, pp. 2599–2601, 1997.

[4] K. D. Choquette, R. P. S. Jr, K. L. Lear, and R. E. Leibenguth, "Gain dependent polarization properties of vertical-cavity lasers," *IEEE J. Select. Topics Quantum Electron.*, vol. 1, pp. 661–666, 1995.

[5] M. Sondermann, M. Weinkath, T. Ackemann, J. Mulet, and S. Balle, "Two-frequency emission and polarization dynamics at lasing threshold in vertical-cavity surface-emitting lasers," Phys. Rev. A, 2003, to be published.

[6] C. J. Chang-Hasnain, J. P. Harbison, and L. T. S. N. G. Florez, "Polarization characteristics of quantum well vertical cavity surface-emitting lasers," *Electron. Lett.*, vol. 57, pp. 163–165, 1991.

[7] M. P. van Exter, M. B. Willemsen, and J. P. Woerdman, "Polarization fluctuations in vertical-cavity semiconductor lasers," *Phys. Rev. A*, vol. 58, pp. 4191–4205, 1998.

[8] K. Panajotov, B. Nagler, G. Verschaffelt, A. Georgievski, H. Thienpont, J. Danckaert, and I. Veretennicoff, "Impact of in-plane anisotropic strain on the polarization behavior of vertical-cavity surface-emitting lasers," *Appl. Phys. Lett.*, vol. 77, no. 11, pp. 1590–1592, 2000.
[9] B. Ryvkin, K. Panajotov, A. Georgievski, J. Danckaert, M. Peeters, G. Verschaffelt, H. Thienpont, and I. Veretennicoff, "Effect of photon-energy-dependent loss and gain mechanisms on polarization switching in vertical-cavity surface-emitting lasers," *J. Opt. Soc. Amer. B*, vol. 16, pp. 2106–2113, 1999.
[10] M. S. Miguel, Q. Feng, and J. V. Moloney, "Light polarization dynamics in surface-emitting semiconductor lasers," *Phys. Rev. A*, vol. 52, pp. 1728–1739, 1995.
[11] J. Martín-Regalado, F. Prati, M. S. Miguel, and N. B. Abraham, "Polarization properties of vertical-cavity surface-emitting lasers," *IEEE J. Quantum Electron.*, vol. 33, pp. 765–783, 1997.
[12] S. Balle, E. Tolkacheva, M. S. Miguel, J. R. Tredicce, J. Martín-Regalado, and A. Gahl, "Mechanisms of polarization switching in single-transverse-mode VCSELs: Thermal shift and nonlinear semiconductor dynamics," *Opt. Lett.*, vol. 24, pp. 1121–1123, 1999.
[13] M. S. Miguel, S. Balle, J. Mulet, C. Mirasso, E. Tolkachova, and J. R. Tredicce, "Combined effects of semiconductor gain dynamics, spin dynamics and thermal shift in polarization selection in VCSEL's," in *Proc. SPIE*, vol. 3944, 2000, pp. 242–251.
[14] J. Martín-Regalado, J. L. A. Chilla, J. J. Rocca, and P. Brusenbach, "Polarization switching in vertical-cavity surface-emitting lasers observed at constant active region temperature," *Appl. Phys. Lett.*, vol. 70, pp. 3350–3352, 1997.
[15] G. Verschaffelt, J. Albert, B. Nagler, M. Peeters, J. Danckaert, S. Barbay, G. Giacomelli, and F. Marin, "Frequency response of polarization switching in vertical-cavity surface-emitting lasers," *IEEE J. Quantum Electron.*, vol. 39, pp. 1177–1186, 2003.
[16] B. S. Ryvkin and A. Georgievskii, "Polarization selection in vcsels due to current carrier heating," *Semiconductors*, vol. 33, no. 7, pp. 813–819, 1999.
[17] T. Ackemann and M. Sondermann, "Characteristics of polarization switching from the low to the high frequency mode in vertical-cavity surface-emitting lasers," *Appl. Phys. Lett.*, vol. 78, pp. 3574–3576, 2001.
[18] D. Lenstra, "On the theory of polarization effects in gas lasers," *Phys. Rep.*, vol. 59, pp. 299–373, 1980.
[19] J. Kannelaud and W. Culshaw, "Coherence effects in gaseous lasers with axial magnetic fields. II. Experimental," *Phys. Rev.*, vol. 141, pp. 237–245, 1966.
[20] W. van Haeringen, "Polarization properties of a single-mode operating gas laser in a small axial magnetic field," *Phys. Rev.*, vol. 158, pp. 256–272, 1967.
[21] C. H. Henry, "Theory of the linewidth of semiconductor lasers," *IEEE J. Quantum Electron.*, vol. QE-18, pp. 259–264, 1982.
[22] L. A. Coldren and S. W. Corzine, *Diode Lasers and Photonic Integrated Circuits*. New York: Wiley, 1995.
[23] M. P. van Exter, A. Al-Remawi, and J. P. Woerdman, "Polarization fluctuations demonstrate nonlinear anisotropy of a vertical-cavity semiconductor laser," *Phys. Rev. Lett.*, vol. 80, pp. 4875–4878, 1998.
[24] H. Lem and D. Lenstra, "Saturation-induced frequency shift in the noise spectrum of a birefringent vertical-cavity surface-emitting laser," *Opt. Lett.*, vol. 22, pp. 1698–1700, 1997.
[25] J. Mulet, C. Mirasso, and M. S. Miguel, "Polarization resolved intensity noise in vertical-cavity surface-emitting lasers," *Phys. Rev. A*, vol. 64, p. 023 817, 2001.
[26] S. Balle, "Simple analytical approximations for the gain and refractive index spectra in quantum-well lasers," *Phys. Rev. A*, vol. 57, pp. 1304–1312, 1998.
[27] M. B. Willemsen, M. U. F. Khalid, M. P. van Exter, and J. P. Woerdman, "Polarization switching of a vertical-cavity semiconductor laser as a kramers hopping problem," *Phys. Rev. Lett.*, vol. 82, pp. 4815–4818, 1999.
[28] G. Giacomelli, F. Marin, and I. Rabbiosi, "Stochastic and bona fide resonance: An experimental investigation," *Phys. Rev. Lett.*, vol. 82, pp. 675–678, 1999.
[29] G. Verschaffelt, J. Albert, M. Peeters, K. Panajotov, J. Danckaert, I. Veretennicoff, H. Thienpont, F. M. Sopra, S. Eitel, R. Hoevel, M. Moser, H. P. Zappe, and K. Gulden, "Polarization switching and modulation dynamics in gain- and index-guided vcsels," *Proc. SPIE*, vol. 3946, pp. 246–257, 2000.
[30] H. Kawaguchi, I. S. Hidayat, Y. Takahashi, and Y. Yamayoshi, "Pitchfork bifurcation polarization bistability in vertical-cavity surface-emitting lasers," *Electron. Lett.*, vol. 31, no. 2, pp. 109–111, Jan. 1995.
[31] M. Travagnin, M. P. van Exter, and J. P. Woerdman, "Influence of carrier dynamics on the polarization stability and noise-induced polarization hopping in surface-emitting semiconductor lasers," *Phys. Rev. A*, vol. 56, pp. 1497–1507, 1997.
[32] M. P. van Exter, R. F. M. Hendricks, and J. P. Woerdman, "Physical insight into the polarization dynamics of semiconductor vertical-cavity lasers," *Phys. Rev. A*, vol. 57, pp. 2080–2090, 1998.
[33] G. Van der Sande, J. Danckaert, I. Veretennicoff, and T. Erneux, "Rate equations for vertical-cavity surface-emitting lasers," *Phys. Rev. A*, vol. 67, p. 013 809, 2003.
[34] J. Martín-Regalado, S. Balle, M. S. Miguel, A. Valle, and L. Pesquera, "Polarization and transverse mode selection in quantum well vertical-cavity surface-emitting lasers: Index- and gain-guided devices," *Quantum Semiclass. Opt.*, vol. 9, pp. 713–736, 1997.
[35] T. Ackemann and M. Sondermann, "Characteristics of polarization switching in vertical-cavity surface-emitting lasers," in *Proc. SPIE*, vol. 4286, 2001, pp. 44–54.
[36] M. Sondermann, T. Ackemann, S. Balle, J. Mulet, and K. Panajotov. Experimental and theoretical investigations on elliptically polarized dynamical transition states in the polarization switching of vertical-cavity surface-emitting lasers. *Opt. Commun.*
[37] J. Danckaert, B. Nagler, J. Albert, K. Panajotov, I. Veretennicoff, and T. Erneux, "Minimal rate equations describing polarization switching in vertical-cavity surface-emitting lasers," *Opt. Commun.*, vol. 201, pp. 129–137, 2002.
[38] F. Prati, P. Caccia, and F. Castelli, "Effects of gain saturation on polarization switching in vertical-cavity surface-emitting lasers," *Phys. Rev. A*, vol. 66, p. 063 811, 2002.
[39] B. S. Ryvkin, E. A. Avrutin, and M. Pessa, "Polarization-dependent intersubband absorption saturation and its effects on polarization selection in vertical cavity surface-emitting lasers," *J. Appl. Phys.*, vol. 93, pp. 2353–2358, 2003.
[40] Y. Matsui, D. Vakhshoori, P. Wang, P. Chen, C.-C. Lu, M. Jiang, K. Knopp, S. Burroughs, and P. Tayebati, "Complete polarization mode control of long-wavelength tunable vertical-cavity surface-emitting lasers over 65-nm tuning, up to 14-mw output power," *IEEE J. Quantum Electron.*, vol. 39, pp. 1037–1048, 2003.

Markus Sondermann was born on August 17, 1974. He received the diploma degree in physics from the Westfaelische Wilhelms-Universitaet Muenster, Germany, in 2000. He is currently working toward the Ph.D. degree in physics at the same university.

His research interests include the polarization dynamics of VCSELs, feedback dynamics of semiconductor lasers, and spatio-temporal effects in lasers.

Michael Weinkath was born on October 30, 1975. He received the diploma degree in physics from the Westfaelische Wilhelms-Universitaet Muenster, Germany, in 2002.

Thorsten Ackemann (M'00) was born on December 11, 1964. He received the diploma degree in physics and the Ph.D. degree from the Westfaelische Wilhelms-Universitaet Muenster, Germany, in 1992 and 1996, respectively.

In 1998 and 1999, through a Feodor-Lynen Fellowship of the Alexander von Humboldt Foundation, he joined the Institut Non Lineaire de Nice, Nice, France, in a post-doctoral position working on spatial structures in broad-area VCSELs. In 2003, he became a Senior Lecturer with the University of Muenster, where he is involved with nonlinear optics and photonics. His particular research interest is self-organization phenomena.